3D chromatin structure remodeling by the FET fusion FUS::DDIT3 in myxoid liposarcoma

Elise Gilson*, Fateme Shabaanpour, Grégory Fettweis, Franck Dequiedt

Laboratory of Gene Expression and Cancer, GIGA-Research Institute, University of Liège (Belgium)

INTRODUCTION

Myxoid liposarcoma (MLPS) is driven by the FUS::DDIT3 fusion oncoprotein, which acts as an aberrant transcription factor. While its transcriptional effects are well described, its impact on 3D chromatin organization remains largely unknown. Chromatin architecture is regulated by the cohesin complex and its loader NIPBL, which can be recruited on chromatin by transcription factors.

The aim of this study is to determine whether FUS::DDIT3 interacts with NIPBL on chromatin and thereby modulates cohesin-mediated genome organization in MLPS.

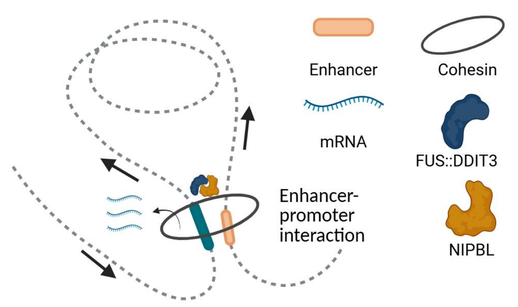

RESULTS

1. GPCA revealed robust interactions between NIPBL and multiple FET fusion proteins, including FUS::DDIT3

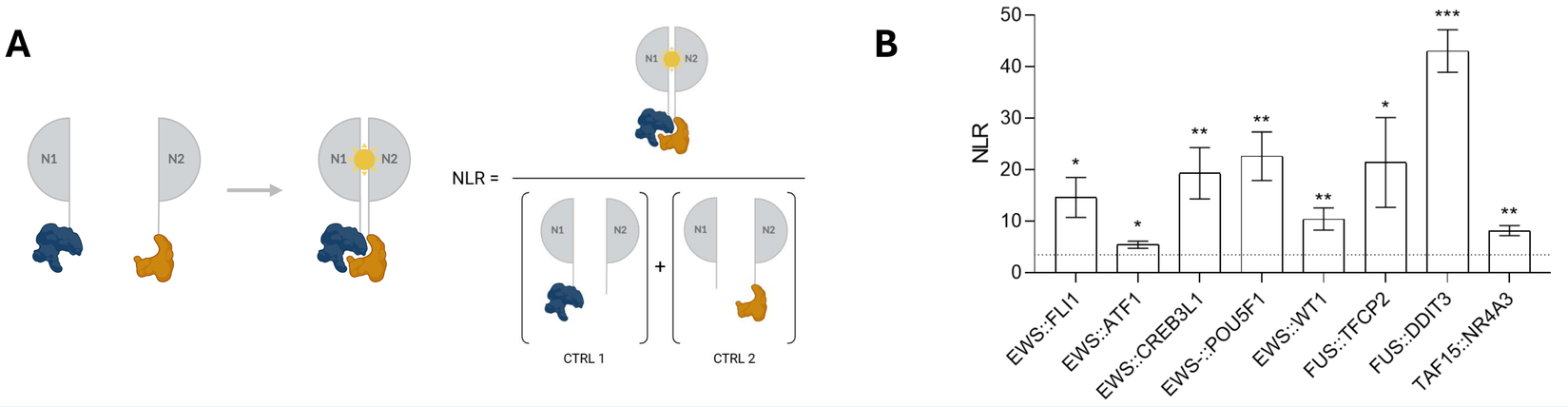

Figure 1. All tested FET fusion proteins interact with NIPBL. (A) Principle of the Gaussian Luciferase Complementation Assay (GPCA). Interaction between proteins fused to complementary Gaussia luciferase fragments (N1/N2) restores luciferase activity, generating a luminescent signal quantified as a normalized luminescence ratio (NLR). **(B)** GPCA between NIPBL and the indicated FET fusion proteins (EWS::FLI1, EWS::ATF1, EWS::CREB3L1, EWS::POU5F1, EWS::WT1, FUS::TFCP2, FUS::DDIT3, and TAF15::NR4A3). Bars show mean NLR ± SEM. The dotted line indicates the background threshold (3.5). Statistical significance was assessed by paired t-test (* $p < 0.05$; ** $p < 0.01$; *** $p < 0.001$).

2. NIPBL and FUS::DDIT3 interact on chromatin with their N and C terminal domains respectively

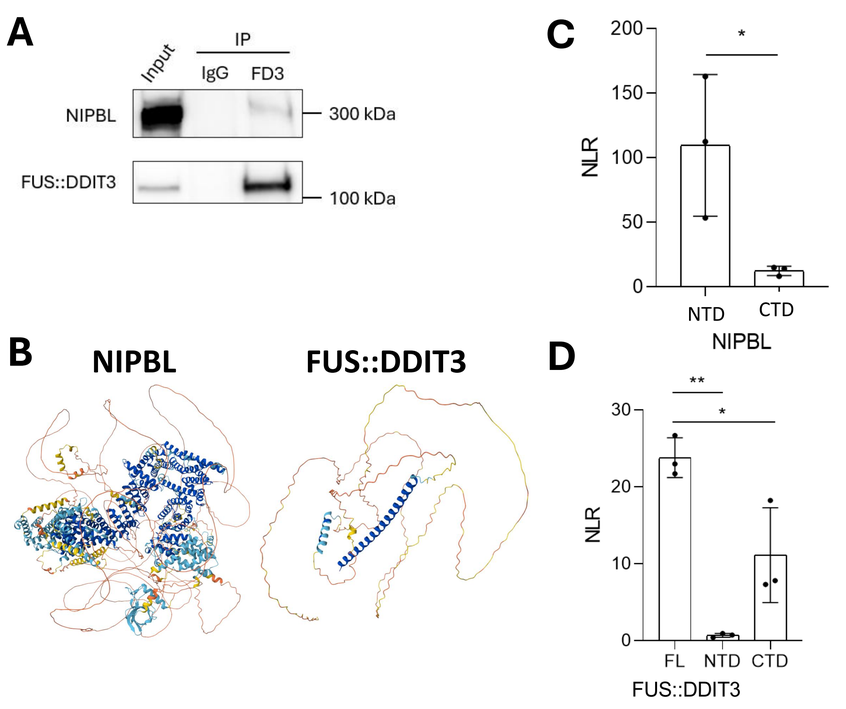

Figure 2. FUS::DDIT3 (FD3) interacts with NIPBL on chromatin. (A) Cell fractionation followed by co-immunoprecipitation was used to assess the FD3-NIPBL interaction in MLS1765. FD3 was immunoprecipitated using anti-DDIT3 or IgG control, and samples were analyzed by western blot. NIPBL and MAU2 were detected in the FD3 immunoprecipitated in the chromatin fraction, with specific enrichment of FD3 compared with IgG. **(B)** Structural models of NIPBL and FUS::DDIT3 generated using AlphaFold. NIPBL displays a predominantly globular architecture, whereas FUS::DDIT3 is largely disordered and contains distinct structured regions, including predicted α-helical segments. **(C)** FD3 preferentially interacts with the N-terminal domain (NTD) of NIPBL compared with its C-terminal domain (CTD). **(D)** The C-terminal domain (CTD) of FD3 preferentially mediates its interaction with NIPBL. Data are shown as individual values with mean ± SD; *$p < 0.05$; **$p < 0.01$.

3. FUS::DDIT3 and NIPBL depletion induce a highly concordant transcriptional response

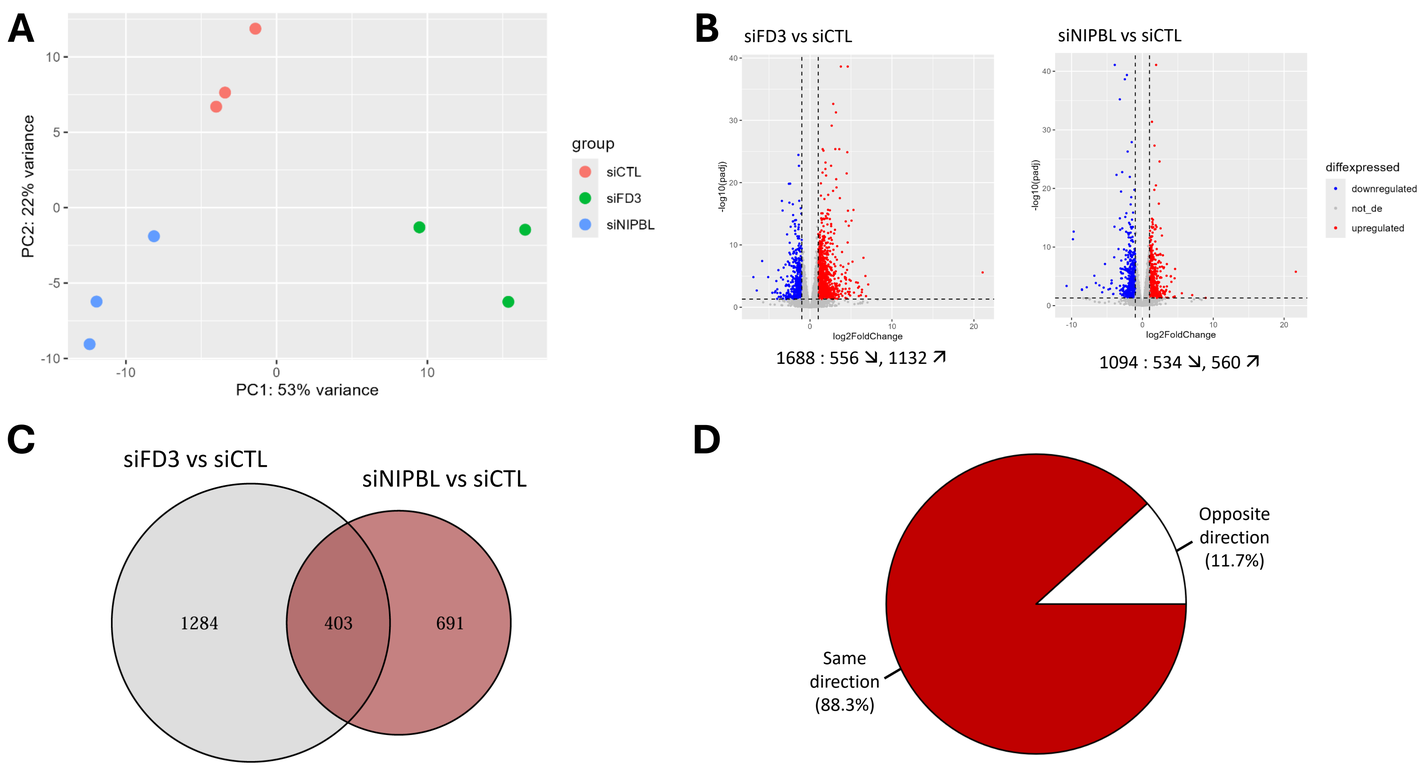

Figure 3. Transcriptomic analysis of FUS::DDIT3- and NIPBL-depleted MLS402 cells. (A) Principal component analysis of RNA-seq samples showing sample clustering according to experimental condition. **(B)** Volcano plots showing differentially expressed genes following FUS::DDIT3 depletion (siFD3 vs siCTL) and NIPBL depletion (siNIPBL vs siCTL). Differentially expressed genes were identified using an adjusted *p*-value < 0.05 and a $|\log_2$ fold-change$|$ > 1. **(C)** Venn diagram showing the overlap between differentially expressed genes identified following FUS::DDIT3 and NIPBL depletion, highlighting the 403 genes commonly regulated by both knockdown. **(D)** Pie chart showing the concordance in the direction of gene expression changes among the commonly regulated genes. 88.3% of genes were regulated in the same direction following FUS::DDIT3 and NIPBL depletion, whereas 11.7% showed opposite regulation.

4. siRNA-mediated depletion of FUS::DDIT3, NIPBL, or the cohesin subunit RAD21 significantly reduced MLPS cells proliferation

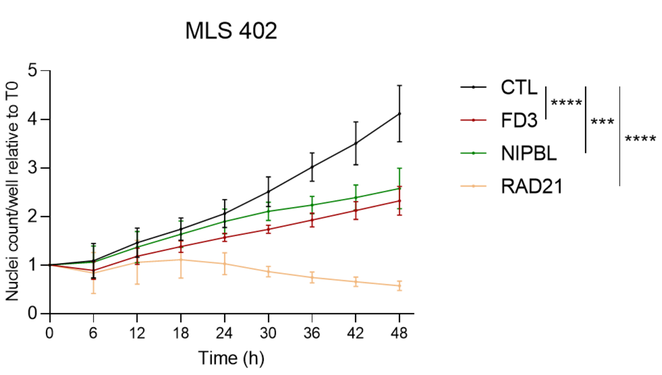

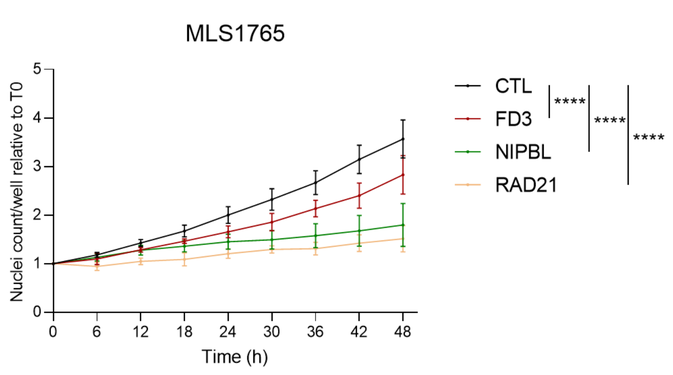

Figure 4. Effect of siRNA-mediated knockdown on cell proliferation. (A) Proliferation curve of MLS402 cells transfected with control siRNA (CTL) or siRNAs targeting FUS::DDIT3 (FD3), NIPBL, or RAD21. **(B)** Proliferation curve of MLS1765 cells under the same experimental conditions. Cell proliferation was monitored over 48 h and quantified as nuclei count per well, normalized to time 0. Data are presented as mean ± SD. Statistical analysis was performed using a two-way repeated measures ANOVA. Significance between conditions is indicated (*** $p < 0.001$; **** $p < 0.0001$).

CONCLUSION

This study identifies NIPBL as an interaction partner of a panel of FET fusions, but more precisely as a chromatin-associated interaction partner of the FUS::DDIT3 fusion oncoprotein in myxoid liposarcoma. Co-immunoprecipitation and GPCA show that FUS::DDIT3 interacts with NIPBL through its C-terminal domain and the N-terminal domain of NIPBL. Transcriptomic analyses reveal substantial overlap between genes deregulated upon FUS::DDIT3 and NIPBL depletion, with mostly concordant expression changes, supporting a functional link. Together, these findings suggest that FUS::DDIT3 may influence 3D chromatin organization through the cohesin-loading machinery, contributing to transcriptional regulation and MLPS cell proliferation.

* Correspondence: elise.gilson@uliege.be